

Characterization of and imprint results using indium tin oxide-based step and flash imprint lithography templates

W. J. Dauksher,^{a)} K. J. Nordquist, D. P. Mancini, D. J. Resnick, J. H. Baker, A. E. Hooper, and A. A. Talin

Motorola Labs, Physical Sciences Research Laboratories, Tempe, Arizona 85284

T. C. Bailey, A. M. Lemonds, S. V. Sreenivasan, J. G. Ekerdt, and C. G. Willson
Texas Materials Institute, University of Texas at Austin, Austin, Texas 78712

(Received 28 May 2002; accepted 16 September 2002)

As compared to quartz relief structures currently employed, indium tin oxide-based (ITO-based) step and flash imprint lithography templates offer advantages in terms of electron-beam writing, scanning electron microscope inspection, and pattern transfer. The material properties of the ITO have been completely characterized, and data is presented for resistivity, crystal structure, transmission, stress, surface roughness, adhesion, composition, and etch characteristics. For a 600 Å annealed ITO film, the resistivity is approximately $3.5 \times 10^2 \Omega/\text{sq}$ and the optical transmission 77% at 365 nm. The atomic film composition was found to be 31.5% In, 4.3% Sn, and 64.2% O by x-ray photoelectron spectroscopy. When contrasted with SiO₂ films, temperature programmed desorption data suggests that hydroxyl groups on the ITO surface bind H₂O less strongly but are more abundant. Ultimate verification of compatibility was obtained by imprinting features into an etch barrier layer using an ITO-based template. The fidelity of 20 nm isolated and semi-isolated features, the smallest features present on the template, was successfully reproduced via the imprinting process. © 2002 American Vacuum Society. [DOI: 10.1116/1.1520575]

I. INTRODUCTION

Step and flash imprint lithography (SFIL) is a relatively new technology that is attractive primarily from the perspectives of low cost, high throughput, and the use of optically transparent templates that can facilitate overlay alignment. It is not inconceivable that SFIL will at least be entertained as a next generation lithography. More likely, though, the strengths of SFIL will be first used for nanofabrication of less complex devices for which high resolution is required. Examples of such devices include filters, waveguides, and photonic crystals.

Early attempts at the fabrication of SFIL templates¹ entailed the use of $6 \times 6 \times 0.25 \text{ in.}^3$ (6025) photomask substrates and leveraged mask shop knowledge of Cr and quartz phase shift etch technology to pattern transfer the substrates. Very recently, the concept of employing an alternative SiO₂/ITO (indium tin oxide)/6025 plate structure has been presented.² Briefly, this form factor is advantageous in that it provides for charge dissipation during electron-beam (e-beam) writing, facilitates inspection by a scanning electron microscope (SEM), and affords a methodology for effectively eliminating microloading effects by relying on the high selectivity of oxide to ITO during a dry etch process.

A plethora of material properties must be satisfied for successful implementation of ITO into the SFIL template structure. From the template fabrication perspective, these properties include: adhesion; stress; resistivity; surface roughness; composition; crystal structure; optical transmission and reflection; and etch characteristics. Requirements

for each of these properties will be discussed along with experimentally determined results.

Further, the imprinting process itself presents additional restrictions on template materials, principally with regards to compatibility with the release layer. The current release layer chemistry was chosen because it works with quartz templates, so the presence of ITO may be significant. In the present work, issues such as release layer durability will be discussed.

Finally, the ultimate verification of ITO-based SFIL template functionality lies in the ability to successfully print features on wafers. Images from one such template are shown, and results of further imprinting studies, including representative critical dimension (CD) data, will be presented in this article.

II. EXPERIMENTAL METHODS

For the fabrication of templates, 600 Å ITO and 1000 Å plasma enhanced chemical vapor deposition (PECVD) SiO₂ films were deposited on 6025 photomask substrates. ZEP520A resist spun to a thickness of 1800 Å was imaged on a Leica VB-6 HR electron-beam exposure system operating at 100 keV. The SiO₂ films were pattern transferred using a CF₄-based reactive ion etch (RIE) process in a Plasma Therm VLR. The remaining e-beam resist was stripped in a conventional barrel asher.

The ITO films themselves were deposited in a Motorola-designed three cathode sputtering system equipped with both radio frequency and direct current sputter capabilities. In this system, the substrate holder is located above the cathodes, and the system base pressure is 5.0×10^{-7} Torr. No presputter surface preparation was performed on the substrates. All

^{a)}Electronic mail: axyx50@motorola.com

depositions were conducted at 3 mTorr and 100 W. In order to maximize optical transmission at 365 nm (the current ideal SFIL exposure wavelength) and to lower resistivity, the ITO films were annealed on a hot plate at 350 °C.

For the purpose of studying ITO film properties, other test substrates including 100 mm round quartz, silicon, and oxidized silicon substrates were also employed. Resistivity measurements were made using a Magnetron four-point probe instrument. X-ray diffraction (XRD) analysis was performed on a Siemens D5000 x-ray diffractometer using a Cu anode. Ultraviolet/visible (UV/Vis) transmission analyses were executed using a Perkin Elmer Lambda 18 UV/Vis spectrometer. For this analysis, ITO samples were prepared on smooth quartz substrates. Percent transmission curves were calculated by referencing the ITO samples to a clean quartz substrate. Stress measurements were taken with a FSM 128 laser deflection radius of curvature tool. Roughness data was obtained in ambient using a Digital Instruments DM3000 scanning probe microscope [atomic force microscopy (AFM)]. The ITO films were imaged in tapping mode using tapping mode etched silicon probes (Digital Instruments) with a nominal tip radius of curvature of 5–10 nm.

X-ray photoelectron spectroscopy (XPS) and temperature programmed desorption (TPD) analyses of ITO and SiO₂ sample surfaces were undertaken using an ultrahigh vacuum (UHV) chamber described in detail elsewhere.³ XPS was performed to determine chemical composition and state using a Perkin Elmer PHI 5000C ESCA system employing Al K α radiation and a spherical capacitance electron kinetic energy analyzer with extended lens optics. The TPD study was conducted in order to estimate the surface concentration of hydroxyl groups to which the template surface treatment (release layer) could bond.

Once completed, the templates were used for imprinting on 200 mm wafers. Prior to imprinting, the templates were cleaned in an ultrasonic acetone bath for 15 min, followed by UV-ozone exposure in a Jelight UVO-42 system for 15 min. The templates were then treated by vapor exposure to tridecafluoro-1,1,2,2-tetrahydrooctyl trichlorosilane (Gelest) at 760 Torr (precursor plus N₂) for 2 h, followed by annealing at 100 °C for 15 min. The imprint template was rinsed with isopropanol and acetone following the surface treatment reaction.

The etch barrier (layer being imprinted) monomers were used as received. The etch barrier was a solution of 4% (w/w) 2-hydroxy-2-methyl-1-phenyl-propan-1-one (Darocur 1173, Ciba) in 1,3-bis(3-methacryloxypropyl)tetramethyldisiloxane (SIB1402.0, Gelest), agitated in a VWR MV-1 vortexer, filtered to 100 nm, and degassed in an ultrasonic bath. Imprinting was performed on an imprint stepper at the University of Texas, which has been described previously.^{4–6}

III. TEMPLATE PROPERTIES

The resistivity of the as-deposited ITO film is on the order of $2.0 \times 10^6 \Omega/\text{sq}$. Figure 1 contains a plot of the change in resistivity as a function of annealing temperature. Below

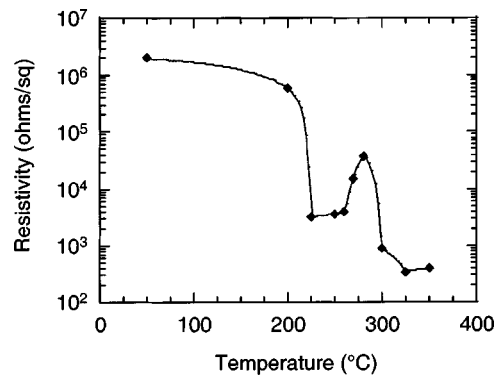


Fig. 1. Plot of resistivity vs bake temperature for a 500 Å ITO film. Sn oxidation and a film phase transformation account for the changes in resistivity.

about 230 °C, the resistivity markedly declines with increasing temperature. This most likely can be ascribed to the oxidation of Sn from the Sn⁺² to the Sn⁺⁴ state.⁷ A second conspicuous change in resistivity occurs over the range of 260–300 °C. As will be seen below, this regime corresponds to the temperature over which an amorphous-to-crystalline phase change of the ITO film is transpiring. In its annealed state, the ITO film resistivity is about $3.5 \times 10^2 \Omega/\text{sq}$. Charge dissipation during e-beam writing and SEM inspection is realized at this conductivity level.

As determined by XRD, the ITO films are amorphous as-deposited. The onset of crystallization begins at 270 °C, and the crystalline peaks, such as the (222) peak at a 2θ of 30.55°, start to become distinguishable. The films are fully crystallized by 300 °C. This data is graphically depicted in the three panels comprising Fig. 2.

Transmission of light through the ITO is quite good. Shown in Fig. 3 are curves of transmission versus wave-

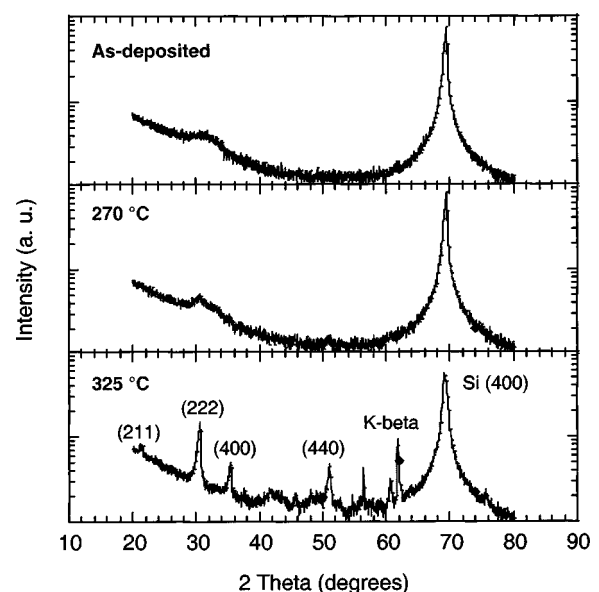


Fig. 2. XRD diffraction intensity plots for an ITO film (top) as-deposited; (middle) annealed to 270 °C; and (bottom) annealed to 325 °C.

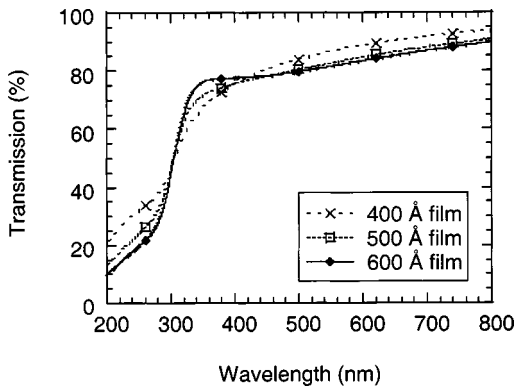


FIG. 3. Transmission spectra for three different thickness ITO films after annealing.

length for three different ITO thicknesses studied. For a 600 Å ITO film, the transmission at 365 nm is approximately 77%. Therefore the use of either a broadband source or an i-line source for exposure should be feasible. The current photocurable polymer has a sensitivity¹ of around 20 mJ/cm². It is anticipated that the reduced light transmission will increase the necessary exposure time, but the final impact on wafer throughput will be very minimal because 20 mJ/cm² is considered to be extremely sensitive when compared to state-of-the-art i-line photoresists.

Mechanical properties of the ITO film are also significant in that they can cause template distortion, film cracking, film bubbling, and the like. For the case of a 600 Å ITO film deposited over 2000 Å SiO₂ on a silicon wafer, the as-deposited stress is, at a value of -6.7×10^9 dynes/cm², somewhat compressive. Annealing causes the stress to become tensile, ultimately reaching a value of 2.0×10^9 dynes/cm². Figure 4 contains the response of film stress with annealing temperature. It can be seen that the most dramatic change in film stress coincides with the regime in which oxidation of Sn from the Sn⁺² to the Sn⁺⁴ state is occurring (temperatures less than 230 °C).

A simple tape test performed on both as-deposited and annealed ITO films indicated that the bond strength to quartz was excellent and no fundamental adhesion issues existed. No lifting was observed.

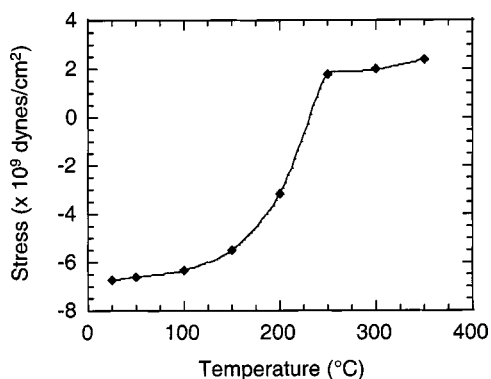


FIG. 4. Stress of a 600 Å ITO film (deposited on 2000 Å TEOS) as a function of annealing temperature.

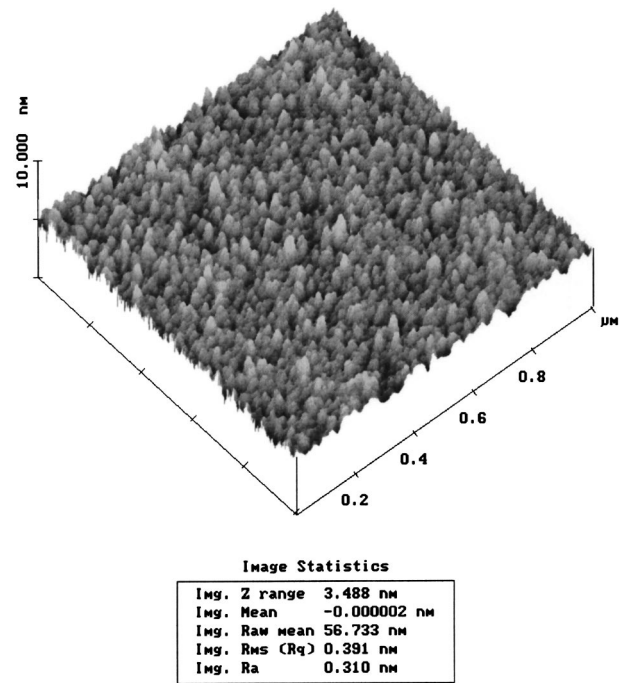


FIG. 5. AFM surface roughness scan for a 500 Å as-deposited ITO film. Peak-to-valley surface roughness is only 3.5 nm (0.4 nm, rms).

Surface roughness, as ascertained via AFM, is shown for a 500 Å thick ITO film in Fig. 5. It can be seen that peak-to-valley surface roughness in the $1 \times 1 \mu\text{m}^2$ scan is only 3.5 nm; the corresponding rms roughness is about 0.4 nm. Furthermore, no inhomogeneous regions are noticed that could, for example, unduly impact template inspection. The roughness increases negligibly (1 nm peak-to-valley) after annealing.

XPS analysis of the ITO film surface (Fig. 6) showed that the In and Sn components were fully oxidized; the binding energies of the In and Sn 3d_{5/2} photoelectron peaks were located at 444.7 and 486.6 eV in accord with published standard values.⁸ Also, no sample charging occurred, indicating that the film was electrically conductive. Using appropriate

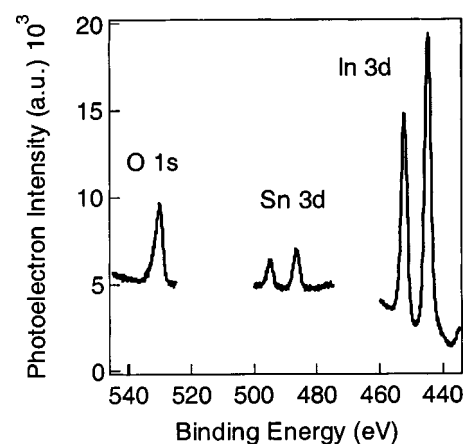


FIG. 6. XPS spectra for the as-deposited ITO thin film after annealing to 423 K to desorb water.

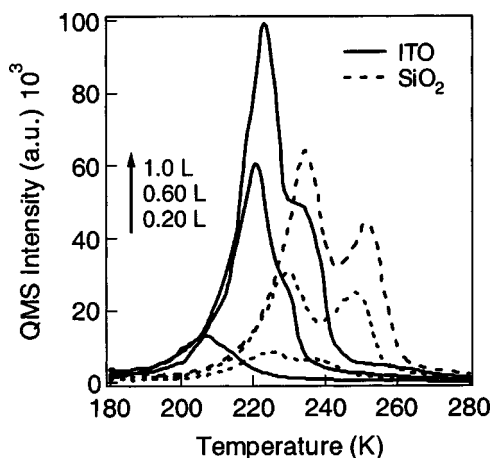


FIG. 7. TPD spectra of the broad desorption feature attributed to hydrogen-bonded CH_3OH for 0.2, 0.6, and 1.0 L exposures on the ITO and SiO_2 surfaces.

sensitivity factors, the atomic composition of the ITO film was determined to be 31.5% In, 4.3% Sn, and 64.2% O.

Finally, the ITO works commendably as an etch stop material. The overlying silicon dioxide can be etched in a fluorine-containing gas such as CF_4 , and neither indium nor tin form volatile fluoride compounds at low temperatures. Sputtering can be kept to a minimum by operating at conditions of low rf bias. In fact, the selectivity between oxide and ITO is greater than 125:1.

IV. ITO COMPATIBILITY

Methanol (CH_3OH) can be used as a probe molecule to determine the surface concentration of hydroxyl ($-\text{OH}$) functional groups on SiO_2 .⁹ When CH_3OH is adsorbed onto SiO_2 at 130 K, it forms hydrogen bonds with the $-\text{OH}$ groups, and the amount of CH_3OH desorbing during a temperature programmed heating ramp titrates the $-\text{OH}$ group density. TPD analyses presented by Sneh and George show multilayer CH_3OH desorption from SiO_2 at 150 K followed by a broad desorption feature from 150 to 220 K, which is attributed to hydrogen-bonded CH_3OH . The integrated peak area of this broad feature is a measure of the density of $-\text{OH}$

groups on the surface. This titration technique was applied in this study to ITO film surfaces for comparison to SiO_2 films deposited by chemical vapor deposition.

Methanol adsorption below 130 K followed by TPD to 423 K was performed for the ITO and SiO_2 surfaces. The mass-to-charge ratio (m/z) 31 (for the CH_3O^+ ionization fragment) was measured by a quadrupole mass spectrometer and used to detect CH_3OH . The samples were annealed at 423 K for 30 min in UHV to desorb water prior to adsorption and TPD procedures. TPD was performed for 0.2, 0.6, and 1.0 L ($1 \text{ L} = 10^{-6} \text{ T s}$) CH_3OH exposures for each sample (Fig. 7), and the TPD spectra for the ITO surface were similar to spectra for CH_3OH desorption from SiO_2 , indicating that this titration method is suitable for detecting $-\text{OH}$ groups on ITO. These exposures do not saturate the $-\text{OH}$ groups; to do this would require at least 100 L exposure⁹ and is beyond the system's capability. Hydrogen-bonded CH_3OH on the ITO sample desorbed about 15 K lower than on the SiO_2 sample, which suggests that CH_3OH was more strongly bound to the hydroxyls on the SiO_2 surface. Relative comparison of TPD peak areas, based upon the average peak area ratio from the exposures examined, showed that the ITO surface had $13 \pm 4\%$ more $-\text{OH}$ groups than the SiO_2 surface. This data suggests that $-\text{OH}$ groups on the ITO surface bind H_2O less strongly than on the SiO_2 surface.

V. IMPRINT RESULTS

In addition to all of the characterization work to qualify the ITO-based templates, confirmation of the feasibility of using these templates was acquired through imprinting studies. SEM images in the etch barrier after imprinting with an ITO-based SFIL template are shown in Fig. 8. Semi-isolated (20 nm lines/150 nm spaces) and isolated lines (20 nm) were successfully imprinted, and these represent the smallest features present on the starting template.

On the templates, sub-100 nm features were found to measure approximately 15 nm over coded sizes. Within the noise of the SEM, the final imprinted images were found to be identical in size (e.g., no imprinting bias) to those found on the templates. Excellent imprint uniformity was also observed. For example, 30 nm semi-isolated features measured 44.6 nm with a 1.5 nm 1σ ; 30 nm isolated features measured

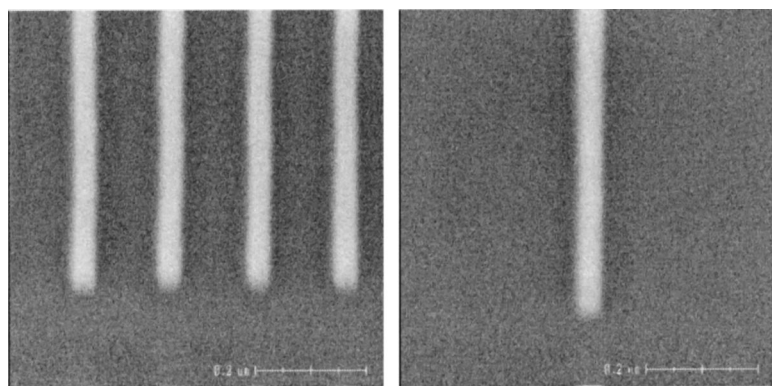


FIG. 8. Images in the etch barrier after imprinting with an ITO-based SFIL template. Shown are 20 nm lines/150 nm spaces (left) and 20 nm isolated lines (right).

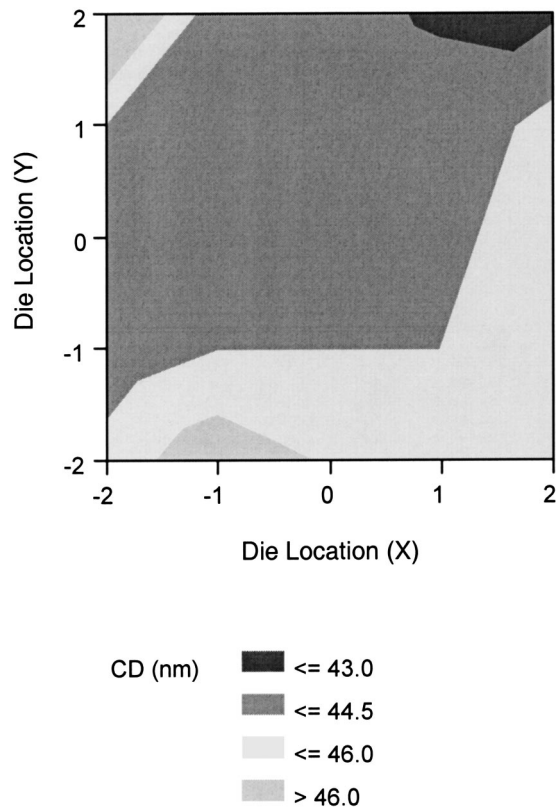


FIG. 9. Contour plot showing uniformity of 30 nm semi-isolated features imprinted on a 200 mm wafer.

45.7 nm with a 1.7 nm 1σ . A contour plot representing CD distribution information for 30 nm semi-isolated imprinted features on 16 dies of a 200 mm wafer can be found in Fig. 9.

Although proof of concept of the use of ITO-based templates has been demonstrated, future work will focus on better tailoring the release layer and/or the release layer preparation sequence to the ITO films. Some larger features did exhibit signs of a potential durability issue. In this context, the TPD data, described above, may be revealing.

VI. CONCLUSION

SFIL offers a low cost, high throughput alternative to other lithographies. A common deficiency for many of the next generation lithographies is the mask structure. We have

presented an ITO-based SFIL template structure that solves many of the problems associated with charging during electron-beam lithography and inspection, as well as with microloading. The ITO films themselves have been rigorously characterized. Proof-of-concept imprints have been performed, generating features as small as 20 nm. Future work will focus on improving compatibility of the release layer with the ITO films so that manufacturing levels of imprints can be performed.

ACKNOWLEDGMENTS

The general support of the staff of Motorola Lab's Physical Sciences Research Laboratories for template fabrication is duly recognized. In particular, the authors would like to thank Eric Newlin for stress measurements and David Standfast for etch processing support. Additionally, the authors appreciate the many hours spent by Anne Dinsmore of Motorola's DigitalDNA™ Laboratories in collecting SEM images and CD data. The authors would also like to thank Steve Johnson, Byung Jin Choi, Matthew Colburn, and the rest of the UT SFIL team for their help in SFIL equipment and process development. Finally, it should be noted that this work was funded in part by DARPA grants (N66001-01-1-8964 and MDA972-97-1-0010) and a SRC contract (96-LC-460).

¹M. Colburn, S. Johnson, M. Stewart, S. Damle, T. Bailey, B. Choi, M. Wedlake, T. Michaelson, S. V. Sreenivasan, J. Ekerdt, and C. G. Willson, *Proc. SPIE* **3676**, 171 (1999).

²T. C. Bailey, D. J. Resnick, D. Mancini, K. J. Nordquist, W. J. Dauksher, E. Ainley, A. Talin, K. Gehoski, J. H. Baker, B. J. Choi, S. Johnson, M. Colburn, M. Meissl, S. V. Sreenivasan, J. G. Ekerdt, and C. G. Willson, *Microelectron. Eng.* **61/62**, 461 (2002).

³K. Yong, P. D. Kirsch, and J. G. Ekerdt, *Surf. Sci.* **440**, 187 (1999).

⁴B. J. Choi, S. Johnson, S. V. Sreenivasan, M. Colburn, T. Bailey, and C. G. Willson, *Proc. ASME DETC2000* **7B**, 861 (2000).

⁵B. J. Choi, S. Johnson, M. Colburn, S. V. Sreenivasan, and C. G. Willson, *Precis. Eng.* **25**, 192 (2001).

⁶T. Bailey, B. J. Choi, M. Colburn, A. Grot, M. Meissl, M. Stewart, J. G. Ekerdt, S. V. Sreenivasan, and C. G. Willson, *Future Electron Dev.* **11**, 54 (2000).

⁷K. Zhang, A. R. Forouhi, and I. Bloomer, *J. Vac. Sci. Technol. A* **17**, 1843 (1999).

⁸J. F. Moulder, W. F. Stickle, P. E. Sobol, and K. D. Bomben, in *Handbook of X-ray Photoelectron Spectroscopy*, edited by J. Chastain (Perkin-Elmer, Eden Prairie, MN, 1992).

⁹O. Sneh and S. M. George, *J. Phys. Chem.* **99**, 4639 (1995).